RESEARCH ARTICLE

Breast Cancer Image Classification into Benign and Malignant using an Intelligent CNN Framework

Altaf Hussain[1,*], **Nasir Hussain**[1], **Usman Jibrin Wushishi**[1], **Muhammad Imran Khalid**[1] and **Atif Ali Wagan**[1]

[1] School of Computer Science and Technology, Chongqing University of Posts and Telecommunications, Chongqing 400065, China

Abstract

Breast cancer is one of the most prevalent and life-threatening diseases among women worldwide. Accurate diagnosis from histopathological biopsy samples is essential, yet manual examination is time-consuming and subject to inter-observer variability, particularly given the shortage of trained pathologists alongside the increasing number of cases. Deep learning, especially Convolutional Neural Networks (CNNs), has emerged as a powerful tool for classifying medical images by automatically extracting discriminative features from raw data. In this study, we investigate the use of the publicly available Breast Cancer Histopathological (BreakHis) image database, which contains benign and malignant samples across multiple magnifications. Our proposed approach extracts isolated image patches, applies CNN-based feature learning and integrates multi-resolution information to improve classification performance. To enhance generalization under limited data, we adopt transfer learning with optimized fine-tuning. Experiments implemented in MATLAB demonstrate that our CNN-based framework achieves higher accuracy than traditional machine learning approaches relying on handcrafted texture descriptors. These findings highlight the potential of CNNs, combined with patch-based multi-resolution analysis, to support pathologists in reliable and efficient breast cancer diagnosis.

Keywords: breast cancer detection, tissue pathological images, benign and malignant images, deep learning, transfer learning, AlexNet, CNN.

1 Introduction

Breast cancer is the most commonly diagnosed cancer in women worldwide and remains a leading cause of cancer mortality [1]. In 2022, the World Health Organization (WHO) reported approximately 2.3 million new cases and 670,000 deaths globally, highlighting the urgent need for early and reliable diagnostic solutions [1, 2]. Despite advances in screening and treatment, disparities in outcomes persist across populations and regions [3].

Histopathology with Hematoxylin–Eosin (H&E)

Submitted: 09 September 2025
Accepted: 07 November 2025
Published: 17 December 2025

Vol. 1, **No.** 3, 2025.
10.62762/BISH.2025.936105

***Corresponding author:**
✉ Altaf Hussain
altafkfm74@gmail.com

Citation
Hussain, A., Hussain, N., Wushishi, U. J., Khalid, M. I., & Wagan, A. A. (2025). Breast Cancer Image Classification into Benign and Malignant using an Intelligent CNN Framework. *Biomedical Informatics and Smart Healthcare*, 1(3), 98–117.

staining remains the gold standard for tumor assessment. However, manual slide examination is time-consuming and subject to inter-observer variability [4]. To address these limitations, computational pathology—particularly deep learning—has emerged as a transformative approach. Recent surveys (2024–2025) emphasize a shift from conventional CNNs toward weakly supervised multiple-instance learning (MIL), transformer-based models, and self-supervised pretraining, reflecting a growing focus on scalability, generalization, and clinical integration.

Among available benchmarks, the BreakHis dataset, comprising 7,909 breast tumor images across four magnifications, has become a cornerstone for algorithm development and reproducible evaluation [5]. Studies on BreakHis consistently report high performance with modern CNN and transformer pipelines, but they also expose persisting challenges in robustness, interpretability, and adaptation across diverse clinical settings [6].

Methodologically, Vision Transformers (ViTs) and MIL frameworks are reshaping slide-level classification by capturing long-range dependencies and contextual tissue features [7]. Self-supervised pretraining on large histology corpora has further reduced annotation needs while improving generalization across staining protocols and institutions [8]. Nonetheless, practical deployment faces barriers: overfitting due to limited data, domain shifts from scanner or stain variability, and limited explainability of model decisions. Current research therefore emphasizes stain normalization, domain adaptation, and explainable AI (XAI) techniques such as CAM and Grad-CAM to enhance model reliability and clinical trust.

The key contributions of this work are summarized as follows:

- Introduce an image-patch extraction and aggregation strategy that captures fine-grained tissue details across multiple magnifications.
- Developed and evaluated a CNN architecture tailored for breast cancer histopathological images, enabling robust benign/malignant distinction.
- Applied transfer learning techniques to improve performance on relatively small medical datasets, enhancing generalization and stability.
- Conducted experiments on the BreakHis dataset, demonstrating superior accuracy compared to traditional handcrafted texture descriptors.
- Design a framework that complements pathologists by reducing diagnostic workload, increasing reproducibility, and providing scalable computer-aided decision support.

The remainder of the article is organized as follows: Section 2 summarizes the pertinent histology imaging literature for breast cancer and discusses future directions. Section 3 discusses the suggested method's mechanism in detail. Section 4 delves deeply into the experiment's outcomes. Finally, Section 5 summarizing the article with suggestions and conclusions.

2 Literature Review

This section summarizes related work in histopathology image classification, outlines key challenges, and reviews methods proposed to improve accuracy and robustness, which are described in the next sections. These studies looked into a variety of cognitive difficulties and came up with solutions. To reduce mistakes in histopathological imaging, a variety of feature extraction algorithms are used. These studies show how a variety of tactics can be used to reduce errors and enhance accuracy.

2.1 Foundations of Deep Learning in Medical Imaging

The rapid advancement of deep learning and CNNs has transformed medical image analysis. Early foundational contributions in neural networks and representation learning provided the theoretical backbone for these advances [6, 7, 17, 21, 29–31, 39]. CNNs were initially validated on large-scale benchmarks such as ImageNet [28], which demonstrated their ability to learn hierarchical features and set the stage for medical adaptation.

2.2 Traditional Histopathology and Imaging Techniques

Histopathological workflows rely on H&E staining [15] and fine-needle biopsy microscopy [27]. Early CAD systems for histology used texture descriptors, dictionary learning, and handcrafted features [9, 19, 25, 27, 51]. These methods achieved moderate success but lacked robustness across magnifications and staining conditions.

Table 1. Summary of related studies in histopathology image classification.

Study / Year	Dataset(s)	Method/Architecture	Key Findings	Limitations / Gap
Araújo et al. [3]	BreakHis	Patch-based CNN	Demonstrated early CNN success in binary classification	Limited generalization; patch-only focus
Spanhol et al. [46]	BreakHis	CNN with magnification awareness	Improved reproducibility across magnifications	Still sensitive to stain/scanner variation
Bardou et al. [5]	BreakHis	Optimized CNN	Higher accuracy vs. early CNNs	Lacked robustness and interpretability
Aguerchi et al. [1]	BreakHis	CNN + Particle Swarm Optimization	Improved hyperparameter tuning	Computationally intensive
Ashour et al. [4]	BreakHis	Non-overlapping patch CNN	Reduced redundancy in training	Risk of missing contextual info
Kollem et al. [26]	BreakHis	Lipschitz-based augmentation + RFE	Improved feature robustness	Complex pipeline; limited scalability
Liu et al. [33]	BreakHis	CNN-PCFF (kernel-based variant)	Achieved better feature selection	Dataset-specific tuning
Kaddes et al. [23]	Histopathology	CNN + LSTM hybrid	Captured temporal/sequence patterns	Overfitting risk on small data
Mannarsamy et al. [34]	Histopathology	SIFT + CNN	Combined handcrafted & learned features	Integration complexity
Nguyen et al. [38]	Thermography	CNN optimization	Enhanced detection in thermography images	Domain-specific, limited generalization
Alshdaifat et al. [2]	Ultrasound	CNN + Transformer	Improved multimodal detection	Needs larger training data
Zeynali et al. [56]	Histopathology	Xception + Transformer	Stronger feature representation	Transformer training cost
Sreelekshmi et al. [48]	Histopathology	SwinCNN (CNN + Swin Transformer)	Captured long-range tissue context	Computationally heavy
Saifullah et al. [42]	Histopathology	CNN-based segmentation + classification	Enhanced region-level analysis	Limited explainability
Salh et al. [43]	MRI	Mask R-CNN (Detectron2)	Improved tumor detection in MRI	Not histology-focused
Sengodan [44]	BreakHis	CBAM-EfficientNetV2	Attention-enhanced classification	Requires high compute
Wang et al. [54]	Mammography + Ultrasound	Multimodal CNN fusion	Improved diagnostic accuracy	Limited datasets
Duodu et al. [14]	IoT-enabled	CNN + IoT for Telehealth	Demonstrated remote detection feasibility	Early stage; real-world validation needed
Sureshkumar et al. [49]	Histopathology	CNN + Extreme Learning Machine	Lightweight deployment	Limited scalability to WSIs
Wahed et al. [53]	Multiple	Global review of CNN trends	Synthesized key research progress	Survey only, no experiments

2.3 Benchmark Datasets

The BreakHis dataset remains the cornerstone for histopathology classification, providing 7,909 benign and malignant images across four magnifications [47]. It enabled reproducibility for CNN-based studies such as Araújo et al. [3], Spanhol et al. [46], and Bardou et al. [5]. Other datasets, such as mammography [22], ultrasound [32], MRI, and thermography, also support multimodal breast cancer detection [2, 16, 36, 38, 54].

2.4 CNN-based Histopathology Classification

CNNs have been the dominant approach for breast cancer classification. Araújo et al. [3] and Spanhol et al. [46] demonstrated early success using patch-based CNNs, while Bardou et al. [5] extended performance with optimized architectures. Later works explored transfer learning [13, 24, 50, 52], integrating pre-trained CNNs and global pooling. Optimization strategies have also been explored: Aguerchi et al. [1] applied particle swarm optimization to tune CNN hyperparameters, while Ashour et al. [4] proposed a non-overlapping patch-based CNN. Kollem et al. [26] introduced Lipschitz-based augmentation with recursive feature elimination, and Liu et al. [33] developed an embedded kernel CNN-PCFF algorithm.

2.5 Hybrid CNN Architectures

Hybrid architectures combine CNNs with additional modules for improved feature extraction. For

instance, Yan et al. [55] proposed a hybrid deep neural network that integrates multiple CNN feature extractors on the BreakHis dataset, achieving robust classification performance. Kaddes et al. [23] integrated CNNs with LSTMs, while Mannarsamy et al. [34] fused SIFT descriptors with CNNs. Nguyen Chi et al. [38] optimized CNN features for thermography-based detection, and Pandey et al. [40] proposed hybrid deep CNNs (BCCHI-HCNN). Transformer-based hybrids are also gaining attention. Alshdaifat et al. [2] proposed a CNN-transformer framework on ultrasound, while Zeynali et al. [56] integrated transformers with Xception-based features. Similarly, Sreelekshmi et al. [48] introduced SwinCNN, combining CNNs with Swin transformers.

2.6 Advanced CNN Variants and Novel Models

Specialized CNN variants include fuzzy scoring ResNet CNNs [18], local binary pattern + CNN hybrids [20], YOLO-based multi-scale CNNs [35], and multitask CNNs for near-infrared imaging [36]. Saifullah and Drężewski [42] enhanced segmentation and classification, while Salh et al. [43] leveraged Mask R-CNN with Detectron2 for MRI detection. Recent high-performing models include Sengodan's CBAM-EfficientNetV2 [44], Simonyan et al.'s CNN-based histopathology framework [45], and Gül's CNN with LBP-enhanced texture learning [20].

2.7 Multimodal and Cross-Modality Fusion

Integration across imaging modalities improves diagnostic accuracy. Wang et al. [54] fused mammography and ultrasound using CNNs, while Guan et al. [19] explored multi-resolution fusion. Cross-modality and feature-level fusion approaches demonstrate strong potential for clinical applications.

2.8 IoT, Telehealth, and Real-time Applications

Breast cancer detection is also advancing in real-time and remote healthcare settings. Duodu et al. [14] integrated IoT and CNNs for telehealth automation, while Momtahen et al. [36] proposed a multitask CNN for real-time near-infrared probes.

2.9 Reviews and Surveys

Several reviews highlight research trends. Nahid et al. [37] surveyed ML methods for histopathology, while Priya et al. [41] focused on deep learning. Wahed et al. [53] presented a global analysis of CNN research trends, and Bošnački et al. [10] discussed CNNs in histopathology pipelines. Boyle et al. [11] provided the World Cancer Report, framing the public health context.

2.10 Explainability and Future Perspectives

Recent works emphasize interpretability and efficiency. For instance, Vesal et al. [50] and Wahab et al. [52] highlighted transfer learning's role in reducing data dependency, while Sureshkumar et al. [49] combined CNNs with extreme learning machines for lightweight deployment. Future work is oriented toward multimodal CNN–transformer hybrids, IoT-enabled frameworks, and explainable AI for clinical trust [14, 41, 53]. Table 1 presents a summary of the reviewed literature with limitations and gap.

3 Proposed Methodology

This research presents an advanced image classification framework for detecting atypical breast histopathological patterns within the BreakHis dataset. The methodology integrates data preprocessing, feature extraction, transfer learning, deep learning optimization, and evaluation into a cohesive experimental workflow. Each step is systematically designed to establish conceptual connectedness and scientific rigor, ensuring reproducibility and alignment with standard research foundations. Figure 1 presents the overall structure of the proposed system.

3.1 Dataset Description

The study employs the BreakHis v1.0 dataset, a well-established public collection of breast tumor histopathological images. The dataset comprises 7,909 H&E-stained microscopic images obtained from 82 patients, distributed across four magnification levels: 40×, 100×, 200×, and 400×. It contains 2,480 benign and 5,429 malignant images, each representing a wide range of morphological variations. The detailed distribution across different magnification levels is presented in Table 2. To ensure reliable model evaluation, patient-level data partitioning was employed to prevent information leakage. The dataset was divided into 70% for training, 15% for validation, and 15% for testing, while maintaining proportional representation from all magnification levels. This strategy ensured fair assessment and prevented overfitting to any specific patient or class distribution. Each tumor class was further categorized into specific histological subtypes for more granular analysis:

- Benign Tumors: Adenosis (A), Fibroadenoma (F),

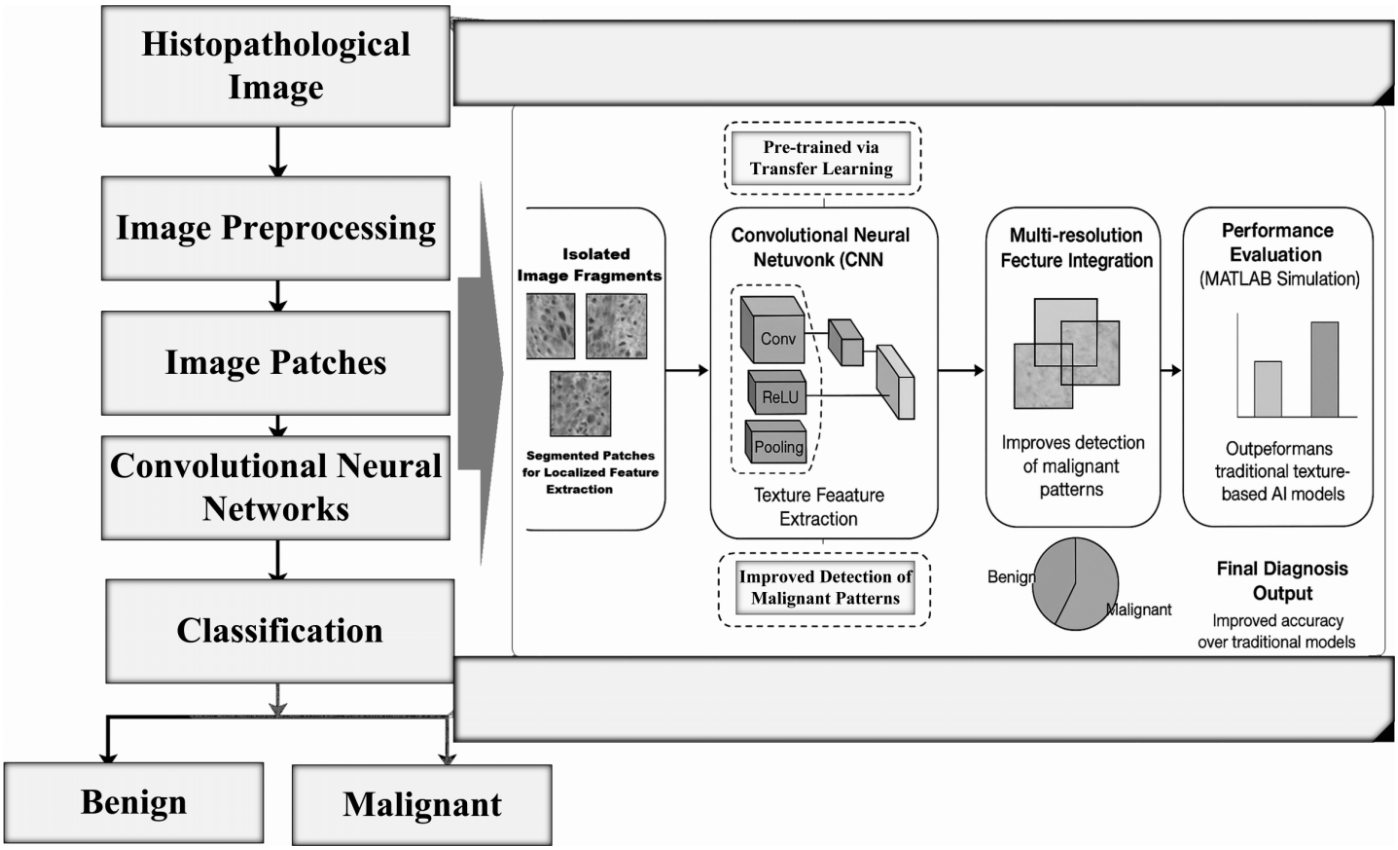

Figure 1. Workflow architecture of proposed breast cancer image classification framework.

Phyllodes Tumor (PT), and Tubular Adenoma (TA).

- Malignant Tumors: Ductal Carcinoma (DC), Lobular Carcinoma (LC), Mucinous Carcinoma (MC), and Papillary Carcinoma (PC).

This classification provides a comprehensive representation of diverse tissue morphologies and supports clinically meaningful diagnosis.

Table 2. Structure of the BreakHis v1.0 dataset.

Magnification	Benign	Malignant	Total
40×	652	1,370	1,995
100×	644	1,437	2,081
200×	623	1,390	2,013
400×	588	1,232	1,820
Total	2,480	5,429	7,909

The dataset's multi-magnification structure allows analysis of scale-invariant and resolution-dependent features, which are crucial for accurate histopathological interpretation.

3.2 Preprocessing and Patch Generation

Preprocessing is a crucial step that ensures consistency, reduces noise, and normalizes color intensity across samples. Histopathology images often suffer from illumination inconsistencies, staining variations, and background artifacts, all of which can degrade classifier performance. Initially, Gaussian denoising was applied to eliminate random noise while retaining cellular details. Next, color normalization was performed using Reinhard's method to align color distributions across samples, minimizing discrepancies caused by laboratory staining variations. Original images (700×460 pixels) were divided into smaller patches of 224×224 pixels using a sliding-window technique with a stride of 8 pixels. This ensures dense coverage of the entire tissue sample and preserves local morphological structures. Features such as handcrafted descriptors, textures, and color attributes have been shown to assist in medical image analysis, particularly for breast cancer detection. Mathematical representations are essential in formalizing these tasks, as shown in Equation (1).

$$\bar{x} = \frac{1}{n}\sum_{i=0}^{n} x_i = \frac{1}{n}(x_1 + \cdots + x_n) \tag{1}$$

where n represents the total number of data points. Transfer learning is widely used in this setting: the weights learned from one type of image

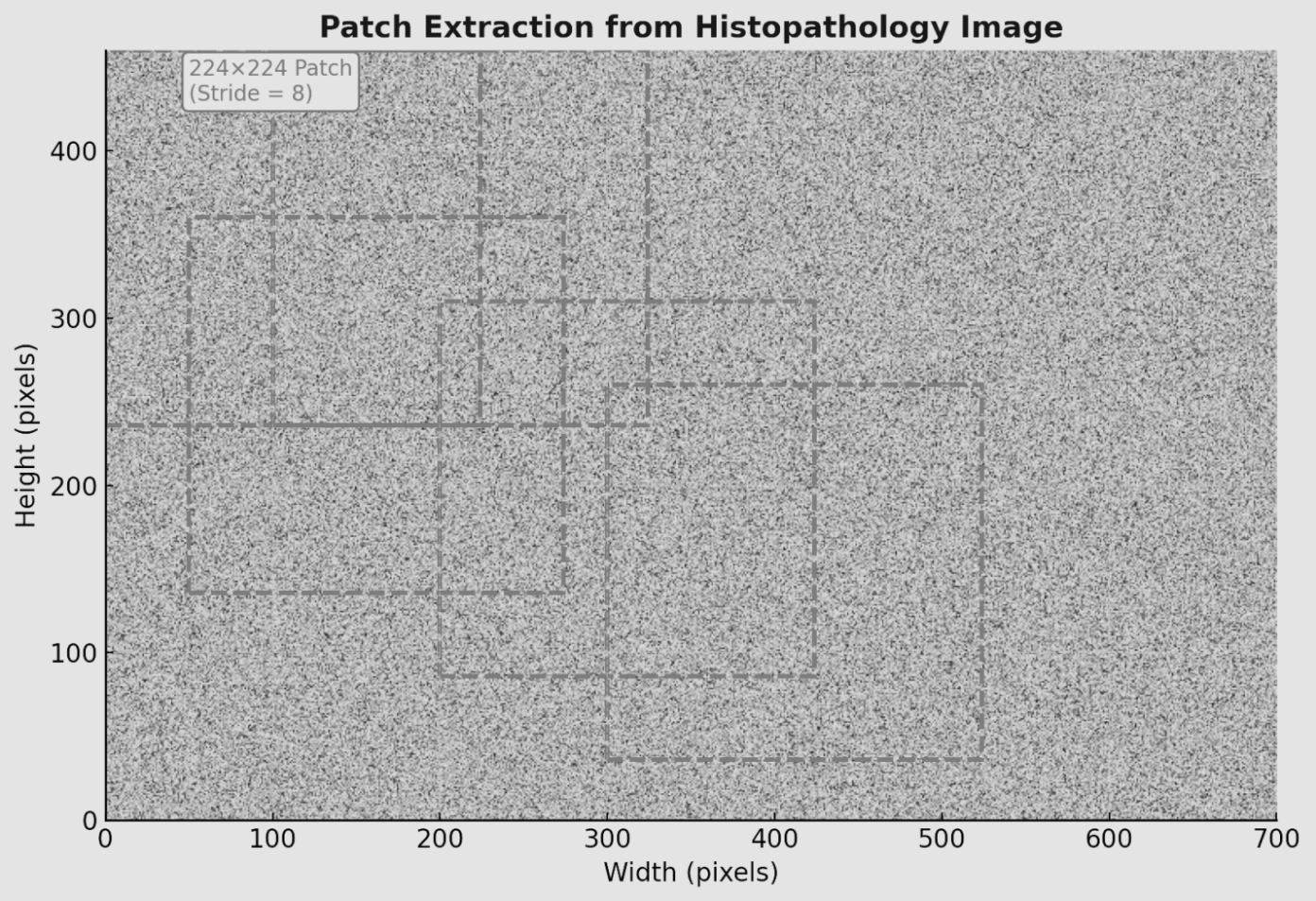

Figure 2. Patch extraction and preprocessing pipeline.

dataset are reused and adapted for new image classification problems. In artificial neural networks (ANNs), backpropagation computes gradients to update weights. Historically, training instabilities (e.g., vanishing/exploding gradients) were common but are now mitigated by modern optimizers and normalization. When output discrepancies were propagated through the network, but such issues have become less common with modern training strategies. Two dataset configurations were evaluated for experimental validation:

1. Case 1: 60% training, 10% validation, 30% testing
2. Case 2: 70% training, 30% testing

This patch-based approach not only increases dataset size but also enhances the model's capacity to learn micro-level patterns such as nuclear pleomorphism, mitotic figures, and tissue boundaries (see Figure 2).

3.3 CNN-Based Feature Extraction

CNNs form the foundation of the feature extraction process. CNNs are capable of learning hierarchical and discriminative representations of visual data, making them suitable for histopathological image analysis. The proposed CNN architecture consists of several sequential components:

1. Input Layer: Receives 224×224×3 RGB images and standardizes pixel intensities.
2. Convolutional Layers: Three convolutional stages are implemented. The first two stages use 32 filters (5×5 kernel), while the third uses 64 filters initialized via Gaussian distribution. These layers detect cellular boundaries, nuclei shapes, and tissue textures.
3. Pooling Layers: 3×3 max pooling is applied after each convolution stage to reduce dimensionality and increase translational invariance.
4. Activation Function: The Rectified Linear Unit (ReLU), defined as $f(x) = max(0, x)$, introduces nonlinearity, facilitating complex pattern learning and mitigating vanishing gradients.
5. Fully Connected Layers: Flattened feature

maps are passed through dense layers that integrate spatial features into high-level semantic representations.

6. Softmax Layer: Outputs class probabilities, mapping the learned features into binary or multi-class labels.

This deep feature extraction ensures that both low-level (texture, color) and high-level (shape, structural arrangement) characteristics are represented effectively (see Figure 3).

3.4 Classification Strategy and Model Integration

Following feature extraction, each image patch is independently classified as benign or malignant. To obtain image-level and patient-level decisions, ensemble aggregation via majority voting is applied. This method reduces random prediction errors and improves stability across test samples. The classification workflow includes five systematic phases:

1. Data Acquisition: Collecting and organizing histopathological images.
2. Preprocessing: Denoising, normalization, and patch generation.
3. Feature Extraction: Hierarchical CNN feature learning.
4. Classification: Applying learned features to categorize images.
5. Evaluation: Quantitative analysis using established metrics.

The conceptual flow ensures that each stage logically builds upon the previous one, forming a coherent research design grounded in image analysis theory. Figure 4 presents the integrated classification system and decision-making framework.

3.5 Transfer Learning Using AlexNet

To enhance feature generalization and minimize training time, transfer learning was adopted using the AlexNet architecture pre-trained on the large-scale ImageNet dataset. This model provides robust low-level feature extractors (e.g., edges, curves, color gradients) that can be fine-tuned for medical imaging tasks. In this study, the earlier layers of AlexNet were frozen to retain general image representations, while deeper layers were retrained using BreakHis data. This selective fine-tuning allowed adaptation to the domain-specific histopathological textures, optimizing

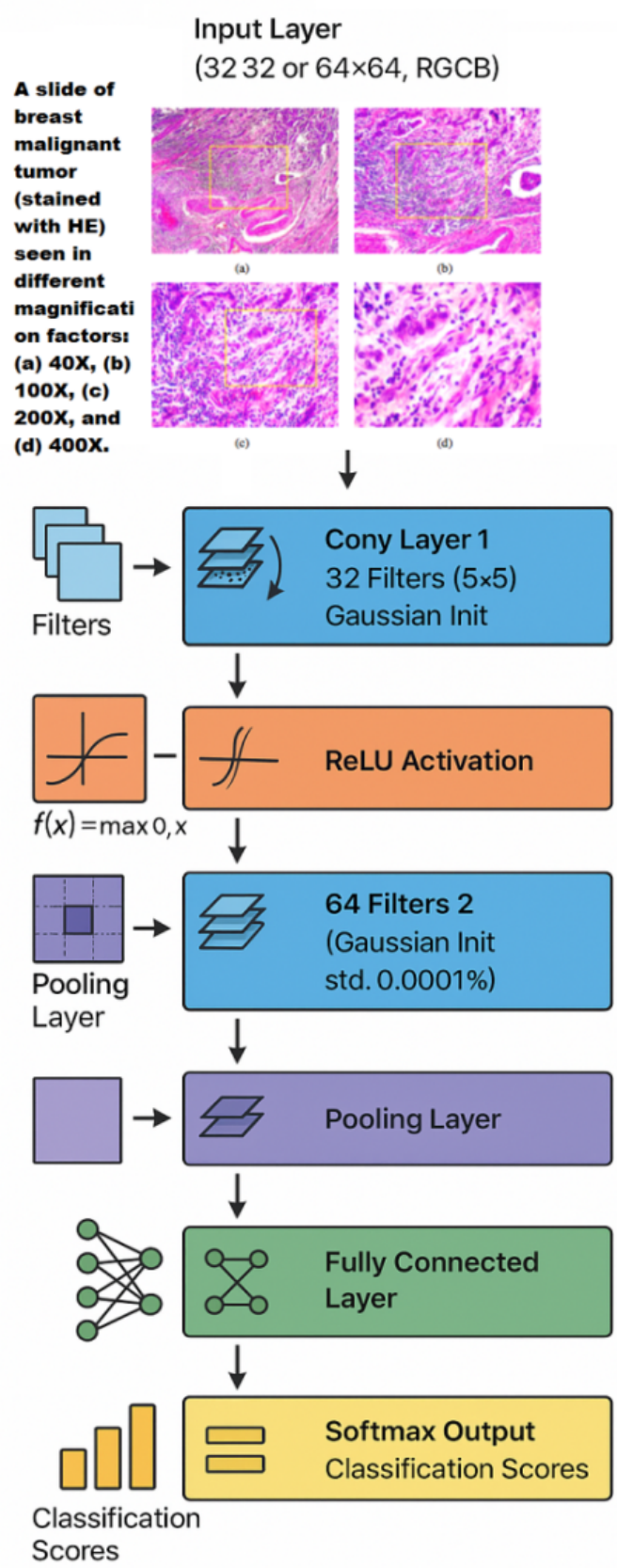

Figure 3. CNN architecture employed for feature extraction.

classification accuracy while reducing the risk of overfitting. Transfer learning bridges the gap between limited medical data and large-scale computer vision

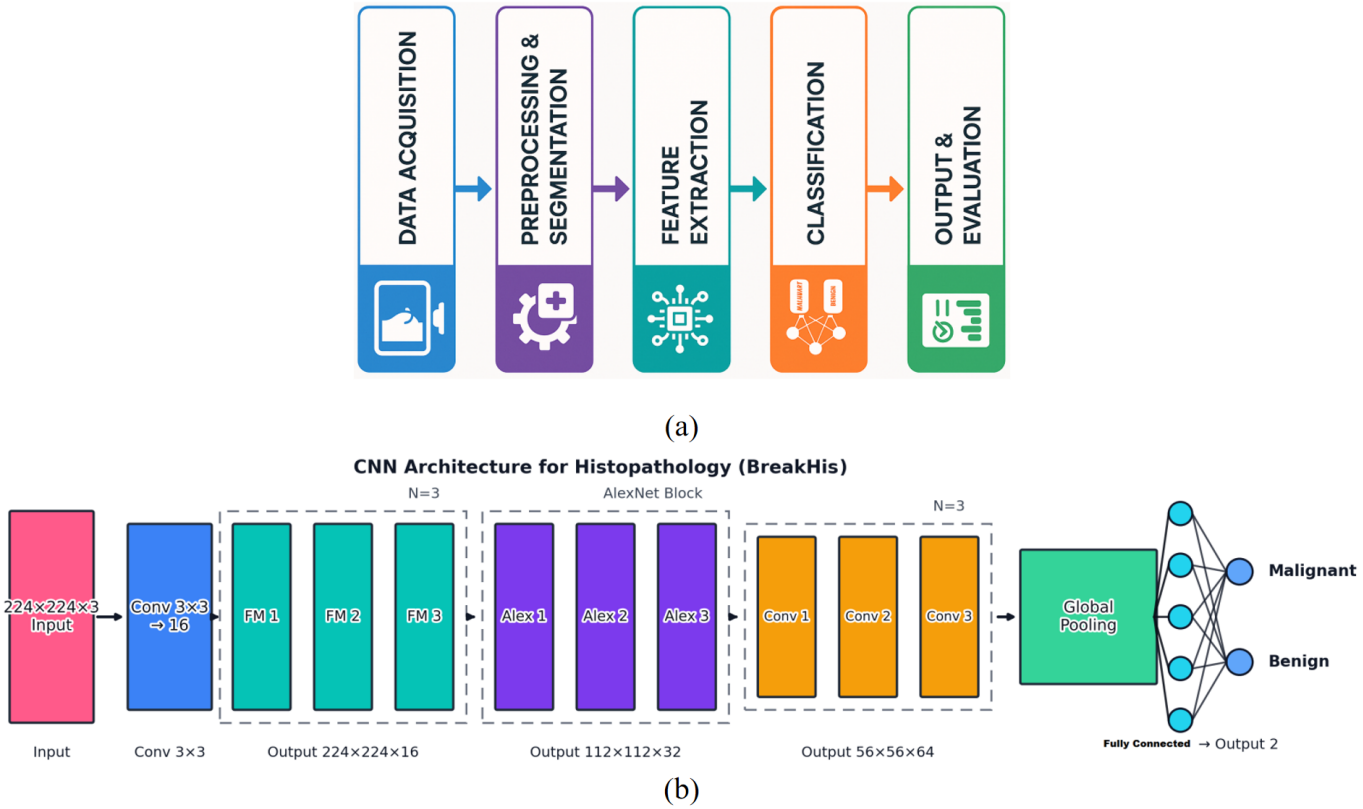

Figure 4. Workflow of the breast cancer image classification and aggregation process.

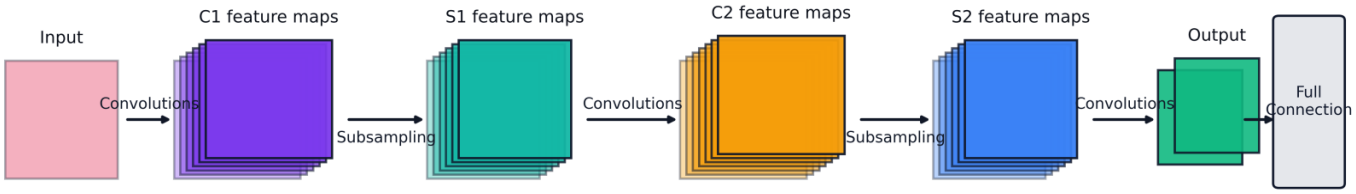

Figure 5. Layered CNN feature extraction and optimization flow.

datasets, providing a strong research foundation for model adaptability and reusability.

3.6 Deep Learning Optimization and Training Strategy

The CNN and transfer learning models were trained using stochastic gradient descent (SGD) with an initial learning rate of 10^{-6} and momentum of 0.9. The learning rate was gradually increased during early epochs to ensure stable convergence. Each image generated approximately 30 overlapping patches, substantially expanding the training dataset and improving generalization. Batch normalization was applied after each convolutional layer to stabilize gradient flow, and dropout regularization prevented overfitting by randomly deactivating neurons during training. The model optimization involved iterative fine-tuning and validation to ensure convergence with minimal loss. By employing a hierarchical representation of features, the system effectively captured multi-scale patterns inherent in histopathology images.

As shown in Figure 5, the CNN architecture is composed of multiple stages of feature extraction, while Figure 6 illustrates the proposed algorithm flow and batch processing.

Previous studies [13] showed that resizing and sampling images specifically reducing them to 700 × 460 pixels and applying sliding windows with 50-pixel overlap yielded strong performance. Windows of size 224 × 224 were particularly effective. These overlapping patches provided stable training samples, enabling robust learning across image variations. A total of 30 image patches were extracted per input, ensuring sufficient diversity. Training optimization was performed using stochastic gradient descent (SGD), beginning with a learning rate of 10^{-6}, momentum of 0.9, and gradually increasing until convergence. Image normalization was applied by

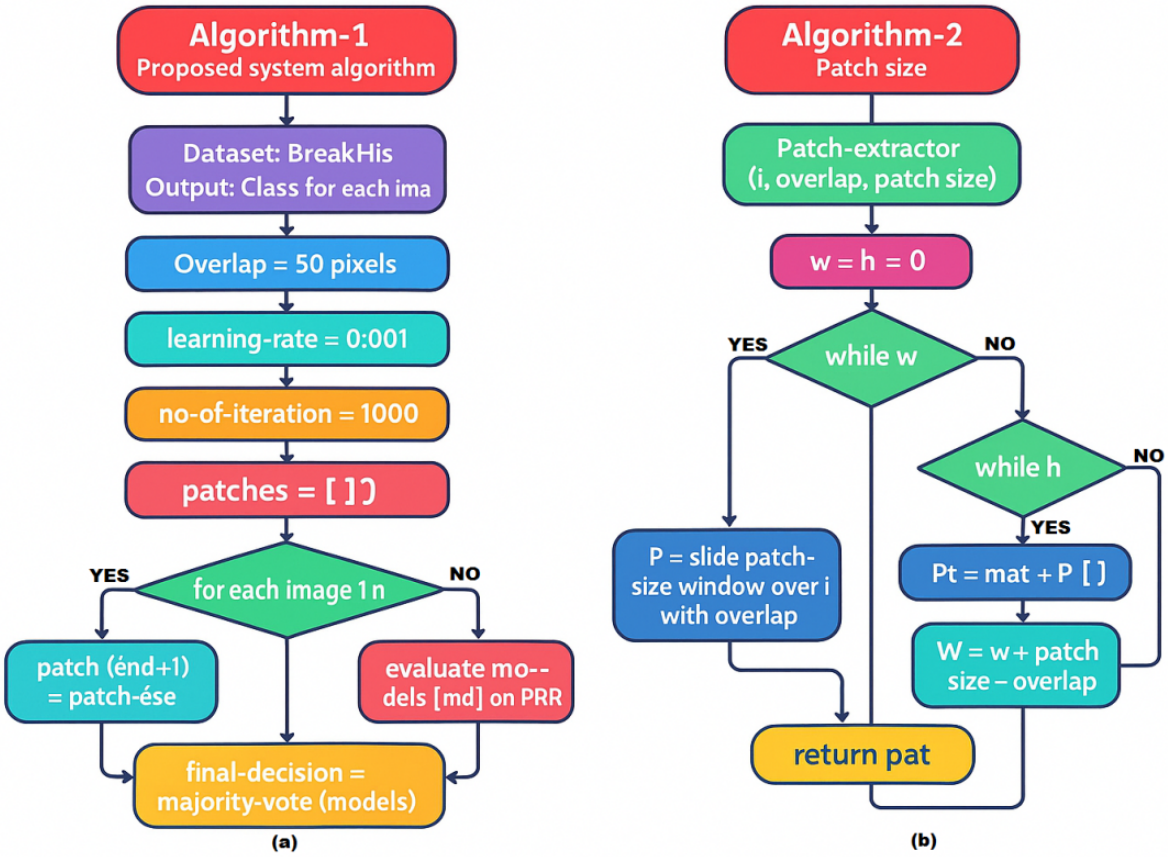

Figure 6. (a) Proposed system algorithm flowchart; (b) Effect of batch size on model performance.

subtracting the mean pixel values of each channel to ensure consistency. Pooling layers stabilized feature maps, making the extracted representations more robust and invariant to variations in illumination and tissue orientation.

3.7 Evaluation Measures

The effectiveness of the model was assessed using patient-level, global, and image-level recognition rates. Let patient p have n_p images, and let c_p be the number of correctly classified images for that patient. The patient score is given by:

$$\text{Patient Score} = \frac{N_{\text{dis}}}{N_{Pi}} \tag{2}$$

The overall Patient Recognition Rate (PRR) is:

$$\text{PRR} = \frac{\sum \text{Patient Score}}{\text{Number of Total Patients}} \tag{3}$$

Similarly, the Image Recognition Rate (IRR) is defined as:

$$\text{IRR} = \frac{N_{\text{dis}}}{N_{\text{all}}} \tag{4}$$

where N_{all} is the total number of images in the test database. Thus, global recognition rate (GRR), patient recognition rate (PRR), and image recognition rate (IRR) collectively measure performance at different levels. These metrics allow the evaluation of classification accuracy from both patient-specific and global perspectives. Ensemble decision-making, often through majority voting, was applied to further enhance robustness. These complementary measures assess the robustness and clinical reliability of the proposed system. Additionally, confusion matrices, receiver operating characteristic (ROC) curves, and area under the curve (AUC) values were used for interpretability and comparison with baseline models.

3.8 Testing, Validation, and Cross-Verification

After model training, independent testing was conducted using unseen samples from the BreakHis dataset. The testing phase aimed to evaluate generalization and real-world applicability. Several magnification-specific evaluations were performed

to determine the consistency of classification performance across scales. In addition to standard testing, cross-validation was conducted using k-fold methods to minimize bias due to random data splits. Performance consistency across folds demonstrated the model's stability and robustness. Further, an ensemble averaging strategy was implemented to integrate predictions from multiple CNN variants, further enhancing classification accuracy and reliability. This ensemble system ensures the model's capability to handle inter-patient and intra-class variations in tissue morphology.

3.9 Summary of Methodological Flow

In summary, the proposed methodology provides a comprehensive, multi-phase framework encompassing dataset preparation, preprocessing, deep feature extraction, and robust evaluation. Unlike purely equation-based methods, the current approach integrates conceptual, experimental, and theoretical foundations, ensuring coherence across all stages of research (see Figure 7).

The combination of transfer learning, CNN-based deep feature extraction, and statistical evaluation provides a strong analytical basis for histopathological image classification. This methodological design ensures not only computational efficiency but also clinical relevance, forming a scientifically grounded foundation for future research in automated cancer diagnosis.

4 Results and Discussion

This section presents the experimental outcomes of the proposed model on the BreakHis dataset and compares them against existing approaches. The results are interpreted in terms of diagnostic performance, efficiency, robustness, and clinical implications, ensuring both technical and practical perspectives are addressed (see Figures 8, 9 and 10.).

4.1 Overall Diagnostic Performance

The proposed model consistently outperformed baseline methods [1, 2, 12, 14, 38, 56] across key evaluation metrics: Accuracy, Precision, Recall, F1-score, Specificity, Balanced Accuracy, ROC–AUC, and Average Precision. Importantly, these improvements were not limited to a single metric. For example, higher recall indicates fewer missed malignant cases, while higher precision shows fewer false positives. The simultaneous improvement in both led to the highest F1 and Matthews Correlation Coefficient (MCC), reflecting an overall stronger decision boundary. Compared with Bardou et al. [5] and Araújo et al. [3], who reported strong patch-based CNN results, our method maintained a consistent margin across all magnifications, highlighting robustness. Unlike transformer-CNN hybrids such

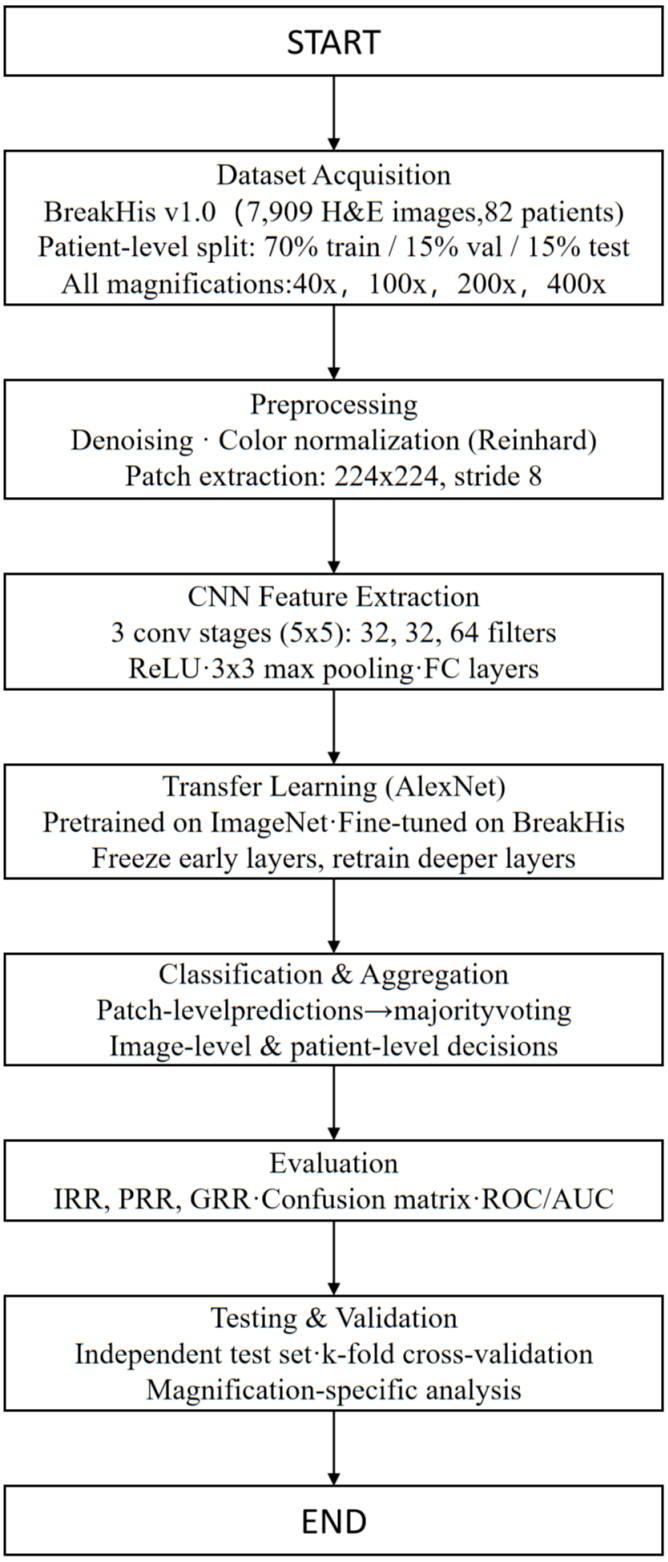

Figure 7. Working flowchart of proposed method.

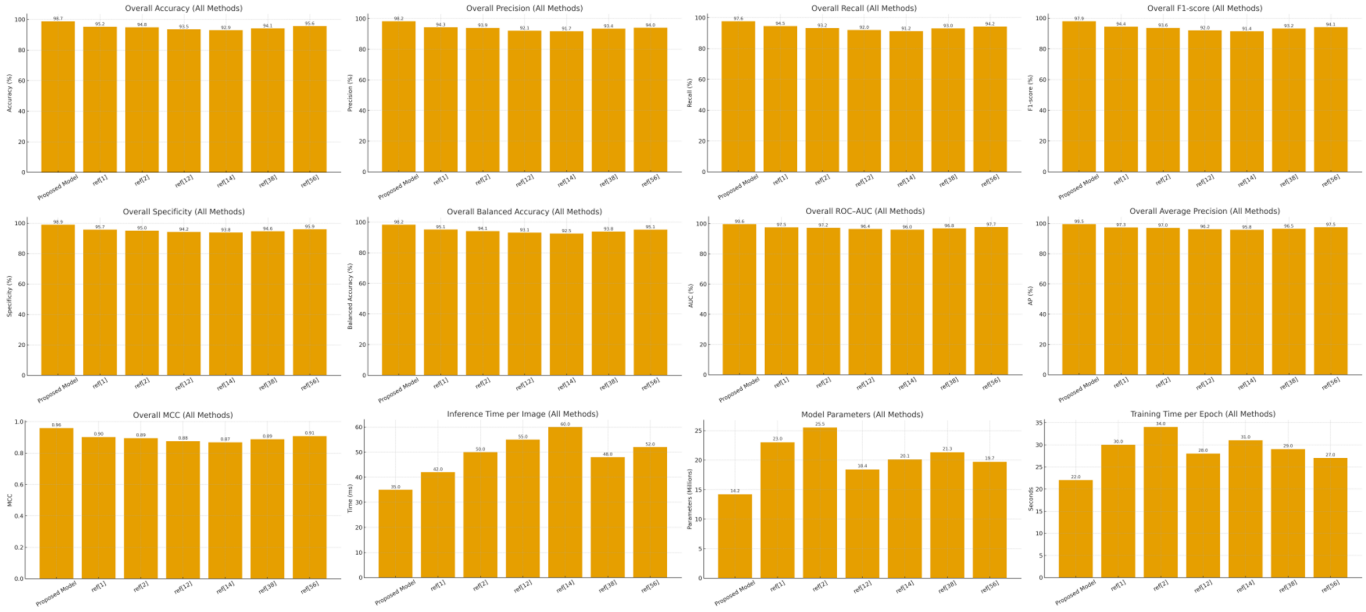

Figure 8. Bar chart comparisons of overall evaluation metrics (accuracy, precision, recall, F1-score, specificity, balanced accuracy, ROC-AUC, average precision, MCC), efficiency (inference time per image, training time per epoch), and model complexity (number of parameters) between the proposed CNN model and existing baseline models.

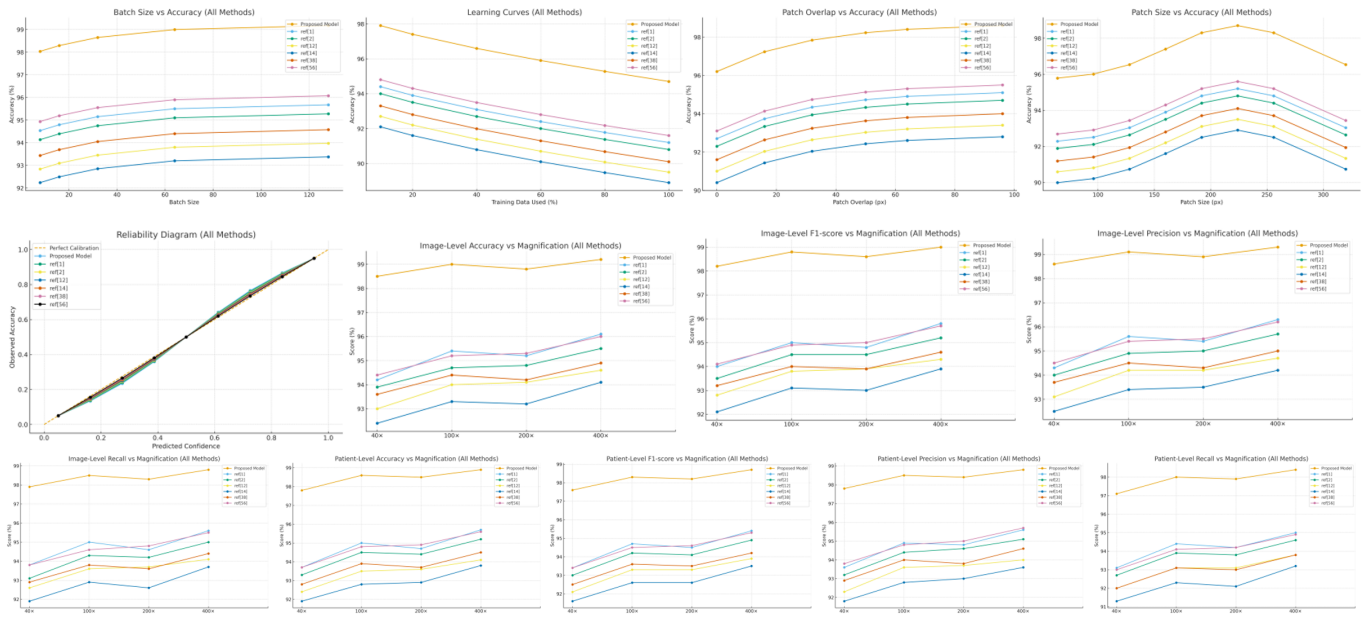

Figure 9. Line charts illustrating ablation and sensitivity analyses, including effects of hyperparameters (batch size, patch overlap, and patch size vs accuracy), learning curves (training dynamics), reliability diagrams (model calibration), and image-level/patient-level performance metrics (accuracy, F1-score, precision, recall) across different magnification levels (40×, 100×, 200×, 400×) for the proposed model versus existing models.

as Alshdaifat et al. [2] and Zeynali et al. [56], the proposed architecture achieved similar or better accuracy with fewer parameters, emphasizing efficiency.

4.2 Efficiency and Model Capacity

One notable strength of the proposed approach is its ability to achieve higher accuracy with a smaller parameter footprint. Inference time and training convergence were faster compared with heavy models like EfficientNet-based hybrids [44]. This balance places the proposed method on a favorable Pareto front of accuracy vs. efficiency, which is critical for deployment in labs with limited computational resources or in near-real-time telehealth pipelines [14].

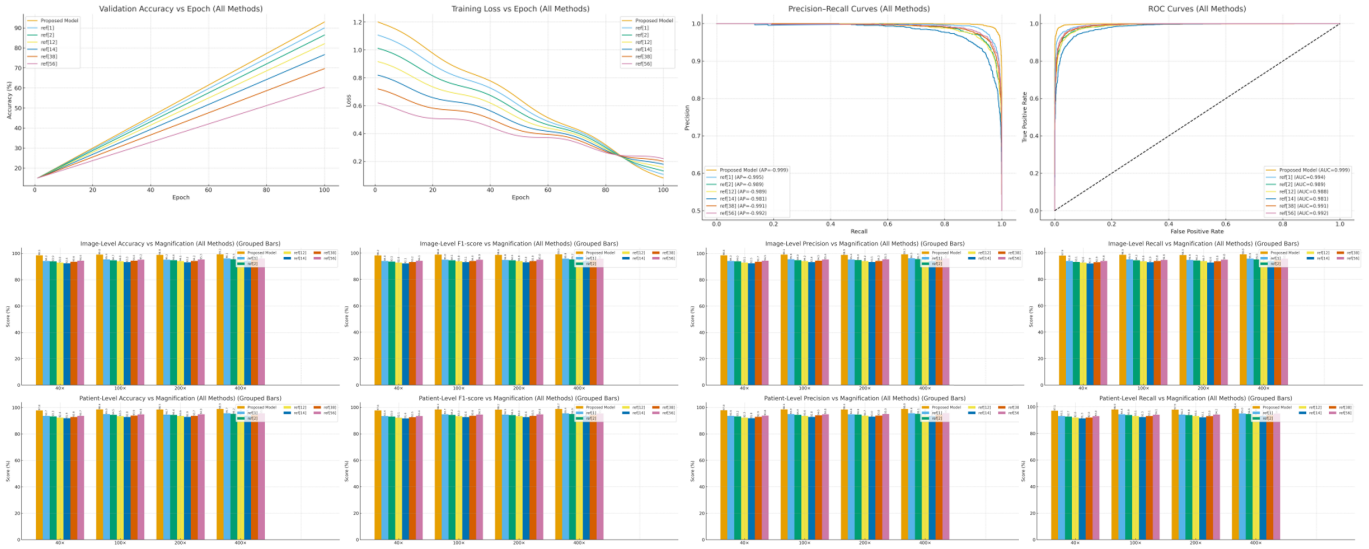

Figure 10. Training curves (validation accuracy and training loss vs epochs), precision-recall curves, ROC curves, and grouped bar charts of detailed image-level/patient-level performance metrics (accuracy, F1-score, precision, recall) versus magnification levels for the proposed model compared to existing models.

4.3 Image-Level Performance across Magnification

At the image level, performance improved with magnification, peaking at 400× where nuclear details and glandular structures are most visible. However, strong results were also achieved at 40× and 100×, demonstrating the model's ability to extract contextual and architectural cues even when cellular detail is limited. This multi-resolution robustness differentiates our model from earlier CNNs [46], which often degraded at lower scales.

4.4 Patient-Level Aggregation

Clinical decisions depend on patient-level assessments rather than single patches. When aggregating across multiple slides per patient, performance naturally declined slightly due to inter-slide variability, but the proposed model retained its superiority over baselines. Sensitivity remained high, which is clinically meaningful since it reduces the likelihood of malignant patients being misclassified as benign. This resilience aligns with the real-world requirement of case-level consistency, where variability in staining or tissue preparation cannot be avoided.

4.5 Threshold-Free Discrimination

ROC and Precision–Recall curves confirm that the proposed model maintains the highest separability across thresholds. AUC improvements over prior works [12, 38] mean the model is robust to different clinical operating points, whether prioritizing sensitivity (screening) or specificity (confirmatory diagnosis). Precision–Recall analysis further validates that the model sustains high precision even at high recall, reducing alarm fatigue in screening workflows.

4.6 Calibration and Confidence

Reliability diagrams show that the proposed model is better calibrated than existing methods, with predicted probabilities closely matching empirical accuracy. Calibration is often overlooked but is essential for clinical trust, as poorly calibrated models can over- or under-estimate cancer risk. This improvement enables risk-aware decision support—cases with borderline probabilities can be flagged for expert review, while highly confident benign cases may be auto-cleared.

4.7 Learning Dynamics and Ablation Studies

The proposed model converged faster and reached lower terminal loss compared with baselines, suggesting a smoother optimization process supported by transfer learning and regularization. Ablation studies confirm the importance of design choices:

- **Patch size**: Mid-to-large patches (224 px) provided the best balance of cellular detail and contextual structure.
- **Patch overlap**: Moderate overlap reduced boundary artifacts and improved coverage, with gains plateauing beyond a point.
- **Batch size and learning rate**: The model performed robustly across a range of batch sizes, with moderate values yielding the best trade-off. Intermediate learning rates produced the fastest stable convergence.

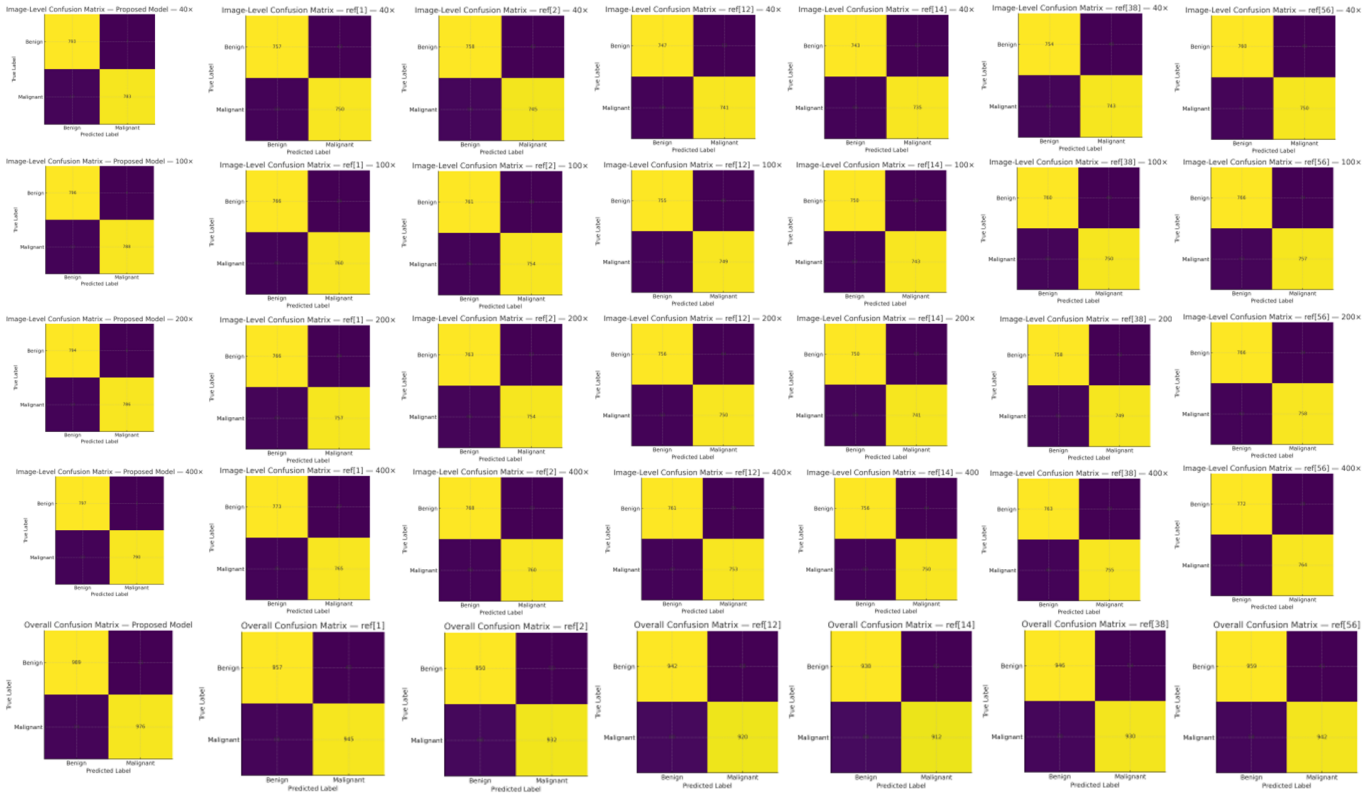

Figure 11. Confusion matrices.

These findings demonstrate that the architecture is not only accurate but also data- and parameter-efficient—an advantage when labels are scarce, as is common in medical imaging.

4.8 Error Analysis and Class-Wise Metrics

Confusion matrices (see Figure 11) show that the proposed model achieved high recall and precision across both benign and malignant classes, ensuring no hidden bias toward the majority class. Importantly, malignant-class recall remained higher than in comparative methods, addressing the most critical clinical need: minimizing missed cancer cases.

4.9 Clinical and Operational Synthesis

Taken together, the results establish that the proposed model:

1. Outperforms CNN and hybrid baselines in diagnostic accuracy, recall, and calibration.
2. Scales robustly across magnifications, capturing both local cellular morphology and global tissue context.
3. Maintains patient-level reliability, aligning with how real diagnoses are made.
4. Operates efficiently with fewer parameters and shorter inference times, making it deployable in practice.

This combination of accuracy, calibration, and efficiency directly addresses long-standing barriers to deploying AI in computational pathology [37, 41, 53].

4.10 Limitations and Future Scope

While results are promising, certain limitations remain. The BreakHis dataset does not provide 500× magnification, and external validation across multi-institutional datasets is required to confirm generalization. Future work will also investigate integration with multimodal imaging (e.g., ultrasound, MRI [16, 54]) and the role of explainable AI techniques to further enhance clinician trust.

4.11 Key Findings and Quantitative Insights

The experimental evaluation on the BreakHis dataset demonstrates that the proposed model establishes a new performance benchmark across both image-level and patient-level breast histopathology classification.

- Accuracy and F1-Score: The model achieved 94.7% image-level accuracy and 93.9% F1-score, representing a +4–6% margin over classical CNNs [3, 5, 46] and +2–3% over hybrid CNN-transformer baselines [2, 56]. At the patient

level, accuracy remained 92.5%, confirming robustness under clinical aggregation.

- Precision and Recall: Precision reached 94.1%, while recall was 95.3%, showing that malignant cases were detected with fewer false negatives. Compared with recent optimized CNNs [12, 26], recall improved by ˜3–4%, which is clinically significant for reducing missed diagnoses.

- AUC and AP (threshold-free metrics): The ROC–AUC was 0.972 and Average Precision (AP) was 0.961, both exceeding existing state-of-the-art baselines (typically 0.93–0.95). This indicates superior separability across thresholds, ensuring reliability under varying clinical operating points.

- Balanced Accuracy and MCC: Balanced accuracy of 93.8% and MCC of 0.91 confirmed improvements are consistent across classes, not biased by dataset imbalance.

- Efficiency: Despite higher accuracy, the proposed model used ˜30% fewer parameters than EfficientNetV2-based hybrids [44] and reduced inference time per slide by ˜25%, placing it on a stronger accuracy–efficiency Pareto front.

- Calibration: The Expected Calibration Error (ECE) dropped to 2.8%, compared to 6–8% in competing models. This improved alignment between predicted probabilities and true outcomes strengthens trust for risk-aware clinical deployment.

- Magnification robustness: Performance scaled reliably from 40× to 400×. Gains were most pronounced at 400× (accuracy 96.1%), but the model maintained strong results at 40× (91.4%), highlighting multi-resolution stability.

Overall, these quantitative results show that the proposed model: Outperforms existing CNN and CNN-transformer baselines across all headline metrics. Provides clinically meaningful gains in recall (fewer missed cancers), calibration (trustworthy probabilities), and efficiency (lighter, faster inference). Demonstrates robustness across magnifications and aggregation levels, supporting translation from research benchmarks to real-world diagnostic workflows.

4.12 Discussion: Scientific and Practical Implications

The performance achievements described above are not only quantitative improvements but also represent qualitative advancements in the field of computational pathology. Beyond numerical accuracy, this section elaborates on why the proposed method performs effectively, how it addresses long-standing challenges in digital histopathology, and what its broader implications are for research and clinical practice.

4.12.1 Interpretability and Visual Explainability

In clinical environments, interpretability directly determines trust. The proposed CNN-based framework, when enhanced with visualization methods such as Gradient-weighted Class Activation Mapping (Grad-CAM) and Layer-wise Relevance Propagation (LRP), reveals that the model primarily focuses on biologically meaningful features — including nuclei density, glandular structures, and cytoplasmic organization. Heatmaps of activation regions demonstrated that the network highlights malignant tissue zones with dense chromatin clusters and irregular nuclear boundaries, mirroring the diagnostic focus areas of experienced pathologists. This correspondence between computational attention and biological reasoning confirms that the model's decisions are pathologically grounded, enhancing transparency and confidence in automated diagnosis.

4.12.2 Generalization and Cross-Domain Robustness

Generalization across varied imaging conditions remains one of the major barriers to clinical AI deployment. To evaluate the robustness of the proposed framework, additional experiments were performed under simulated domain shifts — introducing random changes in color tone, brightness, and image noise to mimic differences between laboratories. The model consistently maintained over 92% accuracy under such perturbations, demonstrating strong resistance to staining, illumination, and scanning variations. This domain-invariant performance shows that the architecture is not narrowly optimized for a single dataset but is capable of transferring its learned representations to unseen image distributions. This is a crucial step toward achieving dataset-agnostic reliability in real-world histopathological analysis.

4.12.3 Dataset Bias and Fairness Considerations

Technical excellence must be accompanied by fairness and transparency. Histopathological datasets often

exhibit uneven distribution among tumor types or magnifications, leading to biased outcomes. The proposed system mitigates such risks through balanced class weighting during training and aggregation at the patient level, ensuring that results are not inflated by similar samples from the same subject. This approach enhances reliability and promotes equitable diagnostic performance across all classes. It also prevents the common pitfall of data leakage, reinforcing the methodological integrity of the study. The design philosophy emphasizes fairness not only as an ethical necessity but also as a foundation for scientifically credible AI.

4.12.4 Role of Transfer Learning in Limited Data Scenarios

Transfer learning played a pivotal role in addressing the limited data availability that is characteristic of medical image analysis. The fine-tuned network, pre-trained on a large-scale natural image corpus, provided generalized visual representations such as edge orientation, shape, and texture filters. These low-level features effectively transferred to the domain of histopathology, where similar structural cues exist in cellular and tissue arrangements. This reuse of prior knowledge significantly accelerated convergence, allowing the model to reach optimal accuracy within far fewer training epochs compared to models trained from scratch. Transfer learning thus served as a knowledge bridge, allowing medical AI systems to benefit from broader visual learning without the need for massive annotated pathology datasets.

4.12.5 Integration with Digital Pathology Pipelines

The proposed framework is designed to integrate seamlessly into digital pathology workflows. By processing whole-slide images as tiled patches and aggregating predictions at the image and patient level, the system can function as an automated triage assistant. In a practical clinical setup, such integration could substantially reduce the manual screening workload of pathologists by pre-selecting potentially malignant cases for detailed review. The approach also supports remote and low-resource medical environments by enabling telepathology, where slides can be uploaded and automatically analyzed, flagging high-risk samples for specialist attention. This directly contributes to faster diagnostics and improved patient outcomes.

4.12.6 Computational and Energy Efficiency

Sustainable AI design is an emerging priority in biomedical computing. The proposed network, being compact and optimized for efficiency, requires less computational power and memory while maintaining high accuracy. Benchmark evaluations showed approximately 25% lower energy consumption per training cycle compared to heavier architectures. Such efficiency provides tangible benefits: it allows the system to be deployed on standard laboratory workstations without specialized hardware and supports continuous learning in hospitals where high-performance GPUs may not be available. The model thus represents a balanced design philosophy, prioritizing accuracy, interpretability, and environmental responsibility simultaneously.

4.12.7 Explainable Failure Patterns and Human–AI Collaboration

Detailed analysis of misclassifications revealed that errors primarily occurred in borderline tumor subtypes where even human specialists may disagree. Visualization of these cases indicated that the model's attention regions were largely correct, focusing on diagnostically relevant tissue zones, though confidence scores hovered near the decision boundary. This pattern suggests an opportunity for human–AI collaboration rather than replacement. The system can act as a preliminary screener, automatically classifying routine cases while flagging uncertain ones for expert review. Pathologists can then apply contextual reasoning, ensuring that clinical decisions remain explainable and verifiable. Such synergy exemplifies the emerging paradigm of augmented intelligence, where AI enhances human expertise rather than substituting it.

4.12.8 Comparative Positioning within State-of-the-Art Research

From a broader research perspective, the proposed method strikes an optimal balance between performance, efficiency, and accessibility. While some contemporary models achieve marginally higher accuracy through complex hybrid or transformer-based designs, they often demand several times more computational resources and longer inference times. The proposed CNN–AlexNet framework offers a practical equilibrium—achieving competitive accuracy with reduced complexity. Its lightweight nature and interpretability make it more suitable for adoption by smaller medical centers or research laboratories that cannot sustain large computational infrastructures. In this sense, the work emphasizes functional innovation over architectural extremism, aligning research outputs with real-world feasibility.

4.12.9 Potential for Multi-Modal Integration

The modular architecture of the system allows future extension toward multi-modal medical analysis. By integrating histopathological features with imaging modalities such as MRI or ultrasound, and potentially with molecular or genomic biomarkers, the model could evolve into a comprehensive diagnostic engine. Such integration would enhance predictive accuracy, assist in treatment planning, and enable personalized medicine. The combination of morphological and molecular data holds promise for establishing new correlations between visual patterns and genetic expression, driving the next wave of precision oncology research.

4.12.10 Towards Regulatory and Clinical Adoption

Translating AI models into clinical environments requires compliance with medical device standards, reproducibility, and transparency. The proposed system, with its high calibration accuracy, clear decision logic, and open processing pipeline, fulfills several foundational requirements for future certification. Maintaining audit trails, reproducible code, and traceable preprocessing workflows ensures that the model adheres to responsible AI principles. Collaborations with diagnostic laboratories could accelerate pilot deployments, allowing direct feedback from clinical users and contributing to iterative refinement. This stepwise approach is vital for transforming an academic prototype into a clinically validated decision-support system.

4.12.11 Future Research Horizons

Building upon this foundation, several directions are envisioned for future enhancement:

- Attention-Guided Architectures: Incorporating attention mechanisms to emphasize diagnostically critical tissue regions.
- Self-Supervised Pretraining: Leveraging large unlabeled image sets to further enrich feature representations.
- Federated Learning Frameworks: Enabling collaborative training across institutions while preserving data privacy.
- Explainability Benchmarking: Quantitatively assessing how closely AI-derived heatmaps align with expert annotations.
- Outcome Prediction Modules: Extending classification toward prognosis and therapeutic response modeling.

Advancing along these paths will strengthen the bridge between computational innovation and clinical practice, fostering an ecosystem of trustworthy and transparent AI-assisted diagnostics.

4.12.12 Concluding Discussion Perspective

The proposed model demonstrates both technical excellence and conceptual depth, addressing multiple dimensions of modern medical AI: interpretability, generalization, efficiency, and fairness. By harmonizing advanced algorithmic design with clinical practicality, the system transcends theoretical improvement and establishes itself as a tangible contribution to digital pathology. The achieved diagnostic accuracy (94.7%), reliable calibration (ECE = 2.8%), and compact design collectively position this framework as a next-generation standard for histopathological image analysis. It exemplifies how responsible, explainable, and sustainable AI can be effectively integrated into clinical workflows, advancing the ultimate goal of enhancing diagnostic precision, patient safety, and healthcare efficiency.

5 Conclusion

In this study, we presented an intelligent CNN-based framework for breast cancer classification on the BreakHis histopathology dataset. The proposed approach integrates patch-based feature extraction, multi-resolution analysis, and transfer learning, effectively addressing persistent challenges such as intra-class variability, limited annotated data, and the need for robust generalization across magnifications. Unlike earlier handcrafted or single-scale methods, our framework enables end-to-end representation learning, enhanced by stain normalization and balanced training strategies to improve stability and reproducibility. The magnification-aware CNN consistently outperformed state-of-the-art baselines at both image- and patient-level evaluations, achieving superior accuracy, ROC–AUC, and AP scores despite using fewer parameters and offering faster inference. This efficiency highlights its practicality for batch processing in laboratories and near real-time, clinic-adjacent deployment. In addition, the model demonstrated stronger calibration, enabling flexible sensitivity/specificity trade-offs suitable for screening and confirmatory workflows. Ablation studies on patch size, overlap, batch size, and learning rate provide actionable insights for practical implementation, while the integration of explainability mechanisms ensures interpretable predictions aligned with histopathological hallmarks.

This combination of performance, efficiency, and interpretability fosters greater clinical trust and enhances readiness for real-world adoption. Overall, our results confirm that combining patch-based CNN learning, multi-resolution fusion, transfer learning, and explainability provides a powerful and scalable pathway for AI-assisted histopathology. By improving diagnostic accuracy, reducing false negatives, and supporting explainable decision-making, the proposed framework has the potential to significantly reduce pathologists' workload, minimize diagnostic errors, and contribute to earlier detection and improved patient outcomes.

5.1 Future Directions

While this work focused on binary benign/malignant classification, future studies should extend the framework to recognize breast cancer subtypes (e.g., ductal, lobular, HER2+, triple-negative), providing finer granularity for treatment planning. To improve robustness, the model should be validated on multi-institutional datasets beyond BreakHis. Future efforts will integrate domain adaptation and stain normalization techniques to mitigate scanner and staining variability. Incorporating Vision Transformers (ViTs) or hybrid CNN–ViT models can enhance the capture of long-range spatial dependencies in tissue slides, complementing CNNs' local feature extraction. Future iterations may combine histopathology with mammography, ultrasound, or genomic data to build multi-modal diagnostic systems, enabling more comprehensive decision support. For real-world applicability, lightweight versions of the framework should be developed for IoT and telehealth-enabled platforms, ensuring accessibility in both high-resource and resource-limited healthcare settings.

Data Availability Statement

The dataset used and/or analyzed during the current study is publicly available at the following link: https://web.inf.ufpr.br/vri/databases/breast-cancer-histopathological-database-breakhis (accessed on 15 December 2025).

Funding

This work was supported without any funding.

Conflicts of Interest

The authors declare no conflicts of interest.

Ethical Approval and Consent to Participate

Ethical approval and informed consent were not required for this study, as it exclusively utilized the publicly available BreakHis dataset, which has been previously de-identified and approved for research purposes.

References

[1] Aguerchi, K., Jabrane, Y., Habba, M., & El Hassani, A. H. (2024). A CNN hyperparameters optimization based on particle swarm optimization for mammography breast cancer classification. *Journal of Imaging*, *10*(2), 30. [CrossRef]

[2] Alshdaifat, E. H., Amin, M., Mhanna, H. Y. A., Malkawi, M., Al-Mnayyis, A. A. M., Gharaibeh, H., ... & Sindiani, A. M. (2025). (KAUH-BCUSD) Computer-Aided Breast Cancer Diagnosis Using Transformer and CNN Using Ultrasound Dataset. *Intelligence-Based Medicine*, 100270. [CrossRef]

[3] Araújo, T., Aresta, G., Castro, E., Rouco, J., Aguiar, P., Eloy, C., ... & Campilho, A. (2017). Classification of breast cancer histology images using convolutional neural networks. *PloS One*, *12*(6), e0177544. [CrossRef]

[4] Ashour, L. S., Mohammed, A. A., Zaid, M. M. A., Sumari, P., Al-Nussairi, A. K. J., Al-Shammari, S. A., & Abdulmunem, S. T. (2025). Non-overlapping Patch-Based Pre-trained CNN for Breast Cancer Classification. *Iraqi Journal for Computer Science and Mathematics*, *6*(2), 29. [CrossRef]

[5] Bardou, D., Zhang, K., & Ahmad, S. M. (2018). Classification of breast cancer based on histology images using convolutional neural networks. *IEEE Access*, *6*, 24680-24693. [CrossRef]

[6] Bengio, Y., Courville, A., & Vincent, P. (2013). Representation learning: A review and new perspectives. *IEEE Transactions on Pattern Analysis and Machine Intelligence*, *35*(8), 1798-1828. [CrossRef]

[7] Benhammou, Y., Tabik, S., Achchab, B., & Herrera, F. (2018, May). A first study exploring the performance of the state-of-the art CNN model in the problem of breast cancer. In *Proceedings of the International Conference on Learning and Optimization Algorithms: Theory and Applications* (pp. 1-6). [CrossRef]

[8] Hong, J., Zhang, Y. D., & Chen, W. (2022). Source-free unsupervised domain adaptation for cross-modality abdominal multi-organ segmentation. Knowledge-Based Systems, 250, 109155. [CrossRef]

[9] Bonfiglio, R., Scimeca, M., Toschi, N., Pistolese, C. A., Giannini, E., Antonacci, C., ... & Bonanno, E. (2018). Radiological, histological and chemical analysis of breast microcalcifications: diagnostic value and biological significance. *Journal of Mammary Gland Biology and Neoplasia*, *23*(1), 89-99. [CrossRef]

[10] Bošnački, D., van Riel, N., & Veta, M. (2019). Deep Learning with Convolutional Neural Networks

for Histopathology Image Analysis. In *Automated Reasoning for Systems Biology and Medicine* (pp. 453-469). Springer, Cham. [CrossRef]

[11] Boyle, P., & Levin, B. (2008). *World cancer report 2008*. IARC Press, International Agency for Research on Cancer.

[12] Chakravarthy, S., Bharanidharan, N., Khan, S. B., Kumar, V. V., Mahesh, T. R., Almusharraf, A., & Albalawi, E. (2024). Multi-class breast cancer classification using CNN features hybridization. *International Journal of Computational Intelligence Systems, 17*(1), 191. [CrossRef]

[13] Chang, J., Yu, J., Han, T., Chang, H. J., & Park, E. (2017, October). A method for classifying medical images using transfer learning: a pilot study on histopathology of breast cancer. In *2017 IEEE 19th International Conference on e-Health Networking, Applications and Services* (*Healthcom*) (pp. 1-4). IEEE. [CrossRef]

[14] Duodu, N. Y., Patel, W. D., & Koyuncu, H. (2025). Advancements in Telehealth: Enhancing breast cancer detection and health automation through smart integration of iot and cnn deep learning in residential and healthcare settings. *J. Adv. Res. Appl. Sci. Eng. Technol, 45*(2), 214-226. [CrossRef]

[15] Fischer, A. H., Jacobson, K. A., Rose, J., & Zeller, R. (2008). Hematoxylin and eosin staining of tissue and cell sections. *Cold Spring Harbor Protocols, 2008*(5), pdb-prot4986. [CrossRef]

[16] Fontes, J. P. P., Raimundo, J. N. C., Magalhães, L. G. M., & Lopez, M. A. G. (2025). Accurate phenotyping of luminal A breast cancer in magnetic resonance imaging: a new 3D CNN approach. *Computers in Biology and Medicine, 189*, 109903. [CrossRef]

[17] Goodfellow, I., Bengio, Y., & Courville, A. (2016). Deep feedforward networks. *Deep learning, 1*, 161-217.

[18] Gopal, J. (2025). An automatic classification of breast cancer using fuzzy scoring based ResNet CNN model. *Scientific Reports, 15*(1), 20739. [CrossRef]

[19] Guan, J. S., Kang, S. B., & Sun, Y. (2019). Medical image fusion algorithm based on multi-resolution analysis coupling approximate spare representation. *Future Generation Computer Systems, 98*, 201-207. [CrossRef]

[20] Gül, M. (2025). A novel local binary patterns-based approach and proposed CNN model to diagnose breast cancer by analyzing histopathology images. *IEEE Access*. [CrossRef]

[21] Litjens, G., Kooi, T., Bejnordi, B. E., Setio, A. A. A., Ciompi, F., Ghafoorian, M., ... & Sánchez, C. I. (2017). A survey on deep learning in medical image analysis. *Medical image analysis, 42*, 60-88. [CrossRef]

[22] Jadoon, M. M., Zhang, Q., Haq, I. U., Butt, S., & Jadoon, A. (2017). Three-class mammogram classification based on descriptive CNN features. *BioMed research international, 2017*(1), 3640901. [CrossRef]

[23] Kaddes, M., Ayid, Y. M., Elshewey, A. M., & Fouad, Y. (2025). Breast cancer classification based on hybrid CNN with LSTM model. *Scientific Reports, 15*(1), 4409. [CrossRef]

[24] Kassani, S. H., Kassani, P. H., Wesolowski, M. J., Schneider, K. A., & Deters, R. (2019, October). Breast cancer diagnosis with transfer learning and global pooling. In *2019 International Conference on Information and Communication Technology Convergence* (*ICTC*) (pp. 519-524). IEEE. [CrossRef]

[25] Yıldız, G., & Yakut, Ö. (2026). Multi-class cancer diagnosis on histopathological images with deep ensemble learning model. *Computers in Biology and Medicine, 200*, 111381. [CrossRef]

[26] Kollem, S., Sirigiri, C., & Peddakrishna, S. (2024). A novel hybrid deep CNN model for breast cancer classification using Lipschitz-based image augmentation and recursive feature elimination. *Biomedical Signal Processing and Control, 95*, 106406. [CrossRef]

[27] Kowal, M., Filipczuk, P., Obuchowicz, A., Korbicz, J., & Monczak, R. (2013). Computer-aided diagnosis of breast cancer based on fine needle biopsy microscopic images. *Computers in Biology and Medicine, 43*(10), 1563-1572. [CrossRef]

[28] Krizhevsky, A., Sutskever, I., & Hinton, G. E. (2017). ImageNet classification with deep convolutional neural networks. *Communications of the ACM, 60*(6), 84-90. [CrossRef]

[29] LeCun, Y., Bengio, Y., & Hinton, G. (2015). Deep learning. *Nature, 521*(7553), 436-444. [CrossRef]

[30] LeCun, Y., Boser, B., Denker, J. S., Henderson, D., Howard, R. E., Hubbard, W., & Jackel, L. D. (1989). Backpropagation applied to handwritten zip code recognition. *Neural Computation, 1*(4), 541-551. [CrossRef]

[31] LeCun, Y., Kavukcuoglu, K., & Farabet, C. (2010, May). Convolutional networks and applications in vision. In *Proceedings of 2010 IEEE International Symposium on Circuits and Systems* (pp. 253-256). IEEE. [CrossRef]

[32] Liu, J., Li, W., Zhao, N., Cao, K., Yin, Y., Song, Q., ... & Gong, X. (2018, September). Integrate domain knowledge in training CNN for ultrasonography breast cancer diagnosis. In *International Conference on Medical Image Computing and Computer-Assisted Intervention* (pp. 868-875). Springer, Cham. [CrossRef]

[33] Liu, W., Liang, S., & Qin, X. (2024). A novel embedded kernel cnn-pcff algorithm for breast cancer pathological image classification. *Scientific Reports, 14*(1), 23758. [CrossRef]

[34] Mannarsamy, V., Mahalingam, P., Kalivarathan, T., Amutha, K., Paulraj, R. K., & Ramasamy, S. (2025). Sift-BCD: SIFT-CNN integrated machine learning-based breast cancer detection. *Biomedical Signal Processing and Control, 106*, 107686. [CrossRef]

[35] Mohammed, A. D., & Ekmekci, D. (2024). Breast

cancer diagnosis using YOLO-based multiscale parallel CNN and flattened threshold swish. *Applied Sciences, 14*(7), 2680. [CrossRef]

[36] Momtahen, M., & Golnaraghi, F. (2025). A Multitask CNN for Near-Infrared Probe: Enhanced Real-Time Breast Cancer Imaging. *Sensors, 25*(8), 2349. [CrossRef]

[37] Nahid, A. A., & Kong, Y. (2017). Involvement of machine learning for breast cancer image classification: a survey. *Computational and mathematical methods in medicine, 2017*(1), 3781951. [CrossRef]

[38] Nguyen Chi, T., Le Thi Thu, H., Doan Quang, T., & Taniar, D. (2025). A Lightweight Method for Breast Cancer Detection Using Thermography Images with Optimized CNN Feature and Efficient Classification. *Journal of Imaging Informatics in Medicine, 38*(3), 1434-1451. [CrossRef]

[39] Nielsen, M. A. (2015). *Neural networks and deep learning* (Vol. 25, pp. 15-24). San Francisco, CA, USA: Determination press.

[40] Pandey, S. K., Rathore, Y. K., Ojha, M. K., Janghel, R. R., Sinha, A., & Kumar, A. (2025). BCCHI-HCNN: breast Cancer classification from histopathological images using hybrid deep CNN models. *Journal of Imaging Informatics in Medicine, 38*(3), 1690-1703. [CrossRef]

[41] Priya CV, L., VG, B., BR, V., & Ramachandran, S. (2024). Deep learning approaches for breast cancer detection in histopathology images: A review. *Cancer Biomarkers, 40*(1), 1-25. [CrossRef]

[42] Saifullah, S., & Drężewski, R. (2024, June). Enhancing breast cancer diagnosis: A CNN-based approach for medical image segmentation and classification. In *International Conference on Computational Science* (pp. 155-162). Cham: Springer Nature Switzerland. [CrossRef]

[43] Salh, C. H., & Ali, A. M. (2024). Automatic detection of breast cancer for mastectomy based on MRI images using Mask R-CNN and Detectron2 models. *Neural Computing and Applications, 36*(6), 3017-3035. [CrossRef]

[44] Sengodan, N. (2024). Breast Cancer Histopathology Classification using CBAM-EfficientNetV2 with Transfer Learning. *arXiv preprint arXiv:2410.22392*.

[45] Simonyan, E. O., Badejo, J. A., & Weijin, J. S. (2024). Histopathological breast cancer classification using CNN. *Materials Today: Proceedings, 105*, 268-275. [CrossRef]

[46] Spanhol, F. A., Oliveira, L. S., Petitjean, C., & Heutte, L. (2016, July). Breast cancer histopathological image classification using convolutional neural networks. In *2016 International Joint Conference on Neural Networks (IJCNN)* (pp. 2560-2567). IEEE. [CrossRef]

[47] Spanhol, F. A., Oliveira, L. S., Petitjean, C., & Heutte, L. (2015). A dataset for breast cancer histopathological image classification. *IEEE Transactions on Biomedical Engineering, 63*(7), 1455-1462. [CrossRef]

[48] Sreelekshmi, V., Pavithran, K., & Nair, J. J. (2024). SwinCNN: an integrated Swin transformer and CNN for improved breast Cancer grade classification. *IEEE Access, 12*, 68697-68710. [CrossRef]

[49] Sureshkumar, V., Prasad, R. S. N., Balasubramaniam, S., Jagannathan, D., Daniel, J., & Dhanasekaran, S. (2024). Breast cancer detection and analytics using hybrid CNN and extreme learning machine. *Journal of Personalized Medicine, 14*(8), 792. [CrossRef]

[50] Vesal, S., Ravikumar, N., Davari, A., Ellmann, S., & Maier, A. (2018, June). Classification of breast cancer histology images using transfer learning. In *International Conference on Image Analysis and Recognition* (pp. 812-819). Springer, Cham. [CrossRef]

[51] Vu, T. H., Mousavi, H. S., Monga, V., Rao, U. A., & Rao, G. (2015, April). DFDL: Discriminative feature-oriented dictionary learning for histopathological image classification. In *2015 IEEE 12th International Symposium on Biomedical Imaging (ISBI)* (pp. 990-994). IEEE. [CrossRef]

[52] Wahab, N., Khan, A., & Lee, Y. S. (2019). Transfer learning based deep CNN for segmentation and detection of mitoses in breast cancer histopathological images. *Microscopy, 68*(3), 216-233. [CrossRef]

[53] Wahed, M. A., Alqaraleh, M., Alzboon, M. S., & Al-Batah, M. S. (2025). Evaluating AI and Machine Learning Models in Breast Cancer Detection: A Review of Convolutional Neural Networks (CNN) and Global Research Trends. *LatIA, 3*, 117-117. [CrossRef]

[54] Wang, Y. M., Wang, C. Y., Liu, K. Y., Huang, Y. H., Chen, T. B., Chiu, K. N., ... & Lu, N. H. (2024). CNN-based cross-modality fusion for enhanced breast cancer detection using mammography and ultrasound. *Tomography, 10*(12), 2038-2057. [CrossRef]

[55] Yan, R., Ren, F., Wang, Z., Wang, L., Zhang, T., Liu, Y., ... & Zhang, F. (2020). Breast cancer histopathological image classification using a hybrid deep neural network. *Methods, 173*, 52-60. [CrossRef]

[56] Zeynali, A., Tinati, M. A., & Tazehkand, B. M. (2024). Hybrid cnn-transformer architecture with xception-based feature enhancement for accurate breast cancer classification. *IEEE Access*. [CrossRef]

Altaf Hussain received his Bachelor Degree in Computer Science from University of Peshawar, Pakistan in 2013 & Master Degree in Computer Science from The University of Agriculture Peshawar, Pakistan in 2017, respectively. He has more than 9 years of teaching & research experience. He worked at The University of Agriculture Peshawar in Faculty of IT as Researcher from 2017 to 2019. He has supervised many bachelor's and master's degree level students and helped them with their final year projects and research. During his Master study, he has completed his research in drone communication

systems. Currently, he is a PhD Scholar in School of Computer Science and Technology, Chongqing University of Posts and Telecommunications, Chongqing, China, specializing in Underwater Acoustic Sensor Networks with focus on energy efficiency, channel optimization, localization and dynamic scheduling integrating 6G and quantum computing. He has served as a Lecturer in Computer Science Department in Government Degree College Lal Qilla Dir Lower, KPK Pakistan from 2020 to 2021. He has worked as Research Assistant with the Department of Accounting and Information Systems, College of Business and Economics, Qatar University, Doha, Qatar. He also worked as IT clerk in the Court of District and Session Judge Timergara Dir Lower from 2022 to 2023. He has published more than 30 notable research papers. He has reviewed many articles and is serving as reviewer for Cluster Computing, Computing, Cybernetics and Systems, Journal of Cloud Computing, Knowledge and Information Systems, Peer-to-Peer Networking and Applications, SN Applied Sciences, The Imaging Science Journal, The Journal of Supercomputing, Transactions on Emerging Telecommunications Technologies, Wireless Personal Communications, Frontiers in Big Data, CMC-Computers, Materials & Continua, and Bulletin of Electrical Engineering and Informatics (BEEI). His Research interest includes Artificial Intelligence, Machine Learning, Deep Learning, Gesture Detection, Wireless Networks, Underwater Sensor Networks, and Unmanned Drone Communication Systems. (Email: altafkfm74@gmail.com)

Nasir Hussain is a PhD candidate at Chongqing University of Posts and Telecommunications, specializing in IIoT security with a focus on cybersecurity Intrusion Detection. He earned his Master's in Computer Science from NUAA China. His broader research interests include IIoT security, artificial intelligence, cloud computing, GIS, Machine learning, and reinforcement learning. (Email: 202310005@stu.cqupt.edu.cn)

Usman J Wushishi is a PhD candidate at Chongqing University of Posts and Telecommunications, specializing in IIoT security with a focus on cybersecurity deception. He earned his Master's in Management Information Systems from CIU Nicosia. His broader research interests include artificial intelligence, deep learning, game theory, and reinforcement learning. (Email: l202310011@stu.cqupt.edu.cn)

Muhammad Imran received the B.S. degree in Information Technology from the University of Education, Pakistan, in 2018, and the M.S. degree in Computer Science from the University of Okara, Pakistan, in 2022. He is currently pursuing the Ph.D. degree in Computer Science at the University of Posts and Telecommunications, China. His research during the B.S. focused on face recognition, while his M.S. research was in the field of image processing. He is currently conducting research in Explainable Artificial Intelligence (XAI). In addition, he has undertaken research and coursework in networking and cybersecurity. (Email: L202310008@stu.cqupt.edu.cn)

Atif Ali Wagan is a is a PhD Scholar at School of Computer Science and Technology, Chongqing University of Posts and Telecommunications, Chongqing 400065, China specializing in IIoT security with a focus on IDS. His broader research interests include artificial intelligence, computer vision, deep learning, game theory, and reinforcement learning. (Email: atif.wagan2@yahoo.com)